10

Simulation of Dendritic Growth in Solidification of Al-Cu alloy by Applying the Modified Cellular Automaton Model with the Growth Calculation of Nucleus within a Cell

Hsiun-Chang Peng and Long-Sun Chao
National Defense University, National Cheng Kung University
Taiwan

1. Introduction

Solidification microstructure is an important index to evaluate the mechanical properties and qualities of the casting. The modeling of microstructure is one of the important aspects of solidification simulation. With the rapid development of computational technique and solidification theory, there is a continuously increasing interest in simulating the microstructure evolution during a solidification process in recent years.

Dendritic microstructure is a common solidification structure whose morphology features affect the properties of product. Dendrite evolution involves the heat, solute transfer and phase transition etc., and these processes always interact with each other, so it is difficult to exactly predict the microstructure evolution. In the past, there are several methods used to simulate the dendrite morphology, including the phase field method, front-tracking method, and the classical and modified cellular automaton methods. The phase field method (Boettinger et al., 2001) has an advantage of dealing with complex topology variation. On the other hand, a phase function has to be introduced into the model that has no much physical meaning. In addition, the mesh size must be smaller than the thickness of interface layer, which limits the computational scale. Furthermore, the thickness of interface layer is a variable that has different values at different positions, which is not consistent with the experiments. The front-tracking method (Juric & Tryggvason, 1996) needs to know the precise position of solid-liquid interface and the velocity of the interface to predict the position of the interface in the next step, so that too much calculation time is consumed on the iteration of the precise interface position.

The classical cellular automaton method (Rappaz & Gandin, 1993; Gandin et al., 1999) has the advantages of simple rules and clear physical backgrounds. Moreover, the mesh size can be much coarser than that of the phase field method. However, the dendrite growth velocity in the method is referenced only to the local temperature in the solidifying region for a fixed alloy composition. Therefore, the individual grains do not interact directly until they touch each other and it is unable to describe the more detail features such as the side branches and the formation of second phases (eutectic). Being different from the classical one, several modified cellular automaton methods (Nastac, 1999; Zhu & Hong, 2001; Beltran-Sanchez &

Stefanescu, 2003) were developed to simulate dendrite morphology with more detailed local conditions, which includes the thermal diffusion and solute redistribution, curvature effect, latent heat release, and the change of solid fraction according to the minute calculation of the growth velocity.

In the presented work, the modified cellular automaton method (Zhu & Hong, 2001) with KGT model is used to simulate the crystal growth of Al-Cu alloy. The mesh size used here is larger than the critical radius of a nucleus. If a mesh (or cell) is chosen as a nucleation site, the growth mechanism is then applied to the mesh instead of regarding it as completely solidified. The directional solidification processes for different solutal concentrations are simulated and compared with the experimental results.

2. Mathematical models

Nucleation. The continuous nucleation condition is considered in the present work where different Gaussian distributions account for the nucleation both on the mold wall and in the bulk liquid. The increase of grain density d_n is induced by an increase in the undercooling $d(\Delta T)$ according to the following Gaussian distribution (Rappaz & Gandin, 1993):

$$\frac{d_n}{d(\Delta T)} = \frac{n_{\max}}{\sqrt{2\pi}\Delta T_\sigma} \exp\left[-\frac{1}{2}\left(\frac{\Delta T - \Delta T_{mn}}{\Delta T_\sigma}\right)^2\right] \tag{1}$$

where ΔT_{mn} is the mean nucleation undercooling, ΔT_σ is the standard deviation, and n_{max} is the maximum density of nuclei given by the integral of this distribution from 0 to ∞. Thus, the density of grains $n(\Delta T)$ formed at any undercooling ΔT is given by

$$n(\Delta T) = \int_0^{\Delta T} \frac{d_n}{d(\Delta T')} d(\Delta T') \tag{2}$$

Growth kinetics and orientation. The growth velocity of a dendrite tip under a certain undercooling ΔT is calculated according to the KGT model (Kurz et al., 1986), which is $v(\Delta T) = k_1\Delta T^2 + k_2\Delta T^3$. k_1 and k_2 are the functions of the initial concentration. The total undercooling at the dendrite tip is given by the sum of the various contributions to undercooling (Rappaz & Gandin, 1993):

$$\Delta T = \Delta T_c + \Delta T_t + \Delta T_r + \Delta T_k \tag{3}$$

where ΔT_c, ΔT_t, ΔT_r, ΔT_k are the solutal, thermal, curvature, and kinetic undercooling, respectively. The kinetic undercooling is small for the metallic alloy under normal solidification, so that the effect is neglected. Nuclei formed on the mold wall or in the bulk liquid grow along the preferential growth direction, which corresponds to 〈10〉 for cubic metals in the present two-dimensional model.

Solute Transport. The local equilibrium at the solid-liquid interface is assumed to balance the interfacial concentrations that are described as follow.

$$C_s^* = kC_l^* \tag{4}$$

where k is the partition coefficient, C_s^* and C_l^* are the interface equilibrium concentrations in the solid and liquid phases, respectively.

As the solidification proceeds, the solidified region rejects solute to the neighboring liquid according to Eq. (4). Diffusion within the entire liquid domain is redistributed by the following equation.

$$\frac{\partial C_l}{\partial t} = \frac{\partial}{\partial x}\left(D_l \frac{\partial C_l}{\partial x} \right) + \frac{\partial}{\partial y}\left(D_l \frac{\partial C_l}{\partial y} \right) + C_l(1-k)\frac{\partial f_s}{\partial t} \tag{5}$$

where D_l is the solute diffusion coefficient in the liquid phase, f_s is the solid fraction, and k is the partition coefficient. The last term of the right hand side of the equation indicates the amount of solute rejected at the solid-liquid interface.
The governing equation for diffusion in the solid phase is given by

$$\frac{\partial C_s}{\partial t} = \frac{\partial}{\partial x}\left(D_s \frac{\partial C_s}{\partial x} \right) + \frac{\partial}{\partial y}\left(D_s \frac{\partial C_s}{\partial y} \right) \tag{6}$$

where D_s is the solute diffusion coefficient in the liquid phase.
Thermal transport. The governing equation for two-dimensional transient heat conduction is

$$\rho C_p \frac{\partial T}{\partial t} = \frac{\partial}{\partial x}\left(\lambda \frac{\partial T}{\partial x} \right) + \frac{\partial}{\partial y}\left(\lambda \frac{\partial T}{\partial y} \right) + \rho \Delta H \frac{\partial f_s}{\partial t} \tag{7}$$

where ρ is the density, C_p is the specific heat, λ is the thermal conductivity, and ΔH is the latent heat.

3. Numerical method

The modified cellular automaton model used to predict the evolution of dendritic structures is based on the coupling of the macroscopic heat and microscopic mass transport. The designation of a nucleus site in a mesh (cell) is followed by applying the growth mechanism to the mesh instead of regarding it as completely solidified.
Nucleation and growth algorithm. The cellular automaton model for the nucleation and growth simulation consists of (1) the geometry of a cell, (2) the state of a cell, (3) the neighborhood configuration, and (4) the transition rule that determines the state of a given cell during any time step. The calculation domain is divided into uniform square arrangement of micromeshes, called cells. Each cell is characterized by different variables such as temperature, concentration, crystallographic orientation, solid fraction and state (i.e. solid or liquid). Two kinds of cells are necessary according to Eq. (5) and (6). One is the liquid cell including the solid-liquid interface and the other is the solid cell. If a cell is a predetermined nucleation cite according to Eq. (1) by the local undercooling, the nucleus in the cell will grow along the preferential direction until the growth touches the boundaries of the cell. Then the state of the cell changes from liquid to solid with a reference index. The cell will grow continuously along the preferential direction corresponding to its crystallographic orientation if the undercooling of any adjacent liquid cell is sufficient to initiate the growth. The growth length L at a given time t_n from the nucleus to the boundaries of nucleation cell or the solid cell to its liquid neighbors can be calculated by

$$L(t_n) = \frac{\left\{ v_1 \left[\Delta T(t_1) \right] \times \Delta t_1 \right\} - r^0 + \sum_{i=2}^{n} \left\{ v_i \left[\Delta T(t_i) \right] \times \Delta t_i \right\}}{\left(\cos\theta + \left| \sin\theta \right| \right)} \tag{8}$$

where Δt_i is the time step size, θ is the angle of the cell's preferential growth direction 〈10〉 with respect to the line between the solid cell to its liquid neighbors or the nucleus to each boundary of the nucleation cell, and n indicates the time step number. r^0 is the critical radius forming a nucleus only effective in the nucleation cell and is zero elsewhere. $v_1\left[\Delta T(t_1)\right]$ and $v_i\left[\Delta T(t_i)\right]$ are the growth rates at time t_1 and t_i. The growth rate in any liquid or nucleation cell can be calculated by using the KGT model depending upon the local undercooling $\Delta T(t_i)$. The neighborhood of 8 cells around a liquid cell is considered to estimate the liquid-to-solid state transition of the liquid cell. The local undercooling $\Delta T(t_i)$ is given by

$$\Delta T(t_i) = T_l - T_{s/l}(t_i) + \left(C_{s/l}(t_i) - C_0\right) - \Gamma \overline{K}_{s/l}(t_i) \tag{9}$$

where T_l is the equilibrium liquidus temperature, m is the liquidus slope, C_0 is the initial concentration, and Γ is the Gibbs-Thomson coefficient. $\overline{K}_{s/l}$, $C_{s/l}(t_i)$ and $T_{s/l}(t_i)$ are the mean curvature, the concentration and the temperature of the solid-liquid interface in the liquid cell at time t_i. Then, the solid fraction $f_s(t_n)$ contributed from a solid cell to the liquid cell at a given time can be expressed as

$$f_s(t_n) = L(t_n) / \ell \tag{10}$$

where ℓ is the length between the solid cell and the liquid cell or half the size (dx/2) of the nucleation cell. Since the neighborhood of 8 cells around a liquid cell is considered, for example, $\ell = dx$ if the solid cell is located at one of the four nearest east, west, south and north neighbors, and $\ell = \sqrt{2}dx$ if the solid cell is located at one of the corner neighbors. When $f_s(t_n) \geqq 1$, which means that the growth front of the solid cell touches the center of the liquid cell.

The transformation of state from liquid to solid depends on the total solid fraction $f_s^t(t_n)$, which can be written as

$$f_s^t(t_n) = \frac{1}{M}\sum_{i=1}^{M} f_s^i(t_n) \tag{11}$$

where M is the total number of the contributed solid neighbors to the liquid cell or total number of the growth components in a nucleation cell. When $f_s^t(t_n) \geq 1$ means that the state of the liquid or nucleation cell changes from liquid to solid and the newly solidified cell gets the same orientation index as the group of the solid cells.

The primary dendrite will grow and coarsen along the preferential 〈10〉 direction by the means of the algorithm described above. As the growing and the coarsening processes of the primary trunk proceed, the solute will be enriched in the liquid near the solid-liquid interface due to the solute redistribution, which will destroy the interface stability and therefore form the side branching or the secondary arms along the primary trunk.

Calculation of the interface curvature. The interface curvature in a cell with the solid fraction f_s is calculated by the counting cell method (Sasikumar & Sreenivasan, 1994), which is expressed as

$$\overline{K}_i = \frac{1}{dx}\left\{1 - \frac{2}{n+1}\left[f_s^t(i) + \sum_{j=1}^{n} f_s^t(j)\right]\right\} \tag{12}$$

where dx is the cell size and n is the number of the neighboring cells. The values of the curvature vary from 1/dx to 0 for convex surfaces and from 0 to -1/dx for concave surfaces.

Calculation of the solute transport. An explicit finite difference scheme is applied for calculating the solute diffusion in both the solid and liquid phases, and the zero-flux boundary conditions are used for the cells located at the surface of the calculation domain. The mesh arrangement is the same as the growth algorithm described above. When a cell transforms its state from liquid to solid by nucleation or growth, its concentration is changed according to Eq. (4). The rejected amount of solute $(C_l^* - kC_s^*)$ will accumulate in the neighboring liquid cell(s).

Solution scheme for macroscopic thermal transport. As the thermal diffusivity of metallic alloys is 3-4 orders of magnitudes greater than the solute diffusivity, the kinetics for microstructure evolution can be assumed to be solute transport-controlled, and therefore the thermal diffusion can be considered to be complete in the microscopic scale. Thus the thermal transport is calculated through the arrangement of macroscopic meshes. The governing equation (Eq. (7)) and related boundary conditions are solved by the explicit finite difference algorithm. The value of temperature simulated is located in the center of the square mesh. The latent heat effect in the last term of Eq. (7) is dealt with by using the temperature recovery method depending on the total variation of the solid fraction in the macroscopic mesh, which is contributed from the change of the liquid-to-solid state in the microscopic cells included. Therefore, the equivalent temperature ΔT_L recovered from a liquid cell due to the latent heat release during nucleation or growth is evaluated by

$$\Delta T_L = \left(\Delta H_V \times dx^2\right) / \left(\rho C_P \times \Delta X^2\right) \tag{13}$$

where ΔH_v is volumetric latent heat release, ρC_p is the volumetric specific heat, and ΔX and dx are the mesh sizes for the macroscopic and microscopic schemes, respectively. Temperature of the macroscopic mesh is then recovered based on Eq. (13) by the newly solidified macroscopic cells. Using these updated temperatures, macroscopic heat transfer calculation can be continued.

Integration of the macroscopic and microscopic schemes. The present model consists of two schemes: the combination of solute transport in FDM and modified cellular automaton model for simulating the evolution of dendritic structures and the macroscopic heat transport in FDM. Based on the calculated temperature profile in the cells, the calculation of nucleation and growth as well as the solute redistribution are carried out by the modified cellular automaton model as described above.

For two different schemes, two kinds of time step are used; one for the macroscopic heat transfer calculation based on the macroscopic mesh, and the other for the modified cellular automaton model, based on microscopic cells, as follows:

Macroscopic time step:

$$\Delta t_{macro} = \left(\Delta X^2 \times \rho C_p\right) / \left(4.5 \times \lambda\right) \tag{14}$$

where λ is the thermal conductivity.
Microscopic time step:

$$\Delta t_{micro} = (1/4.5)\min\left[(dx/V_{\max}),\left(dx^2/D_l\right)\right] \tag{15}$$

where V_{max} is the maximum growth velocity within all liquid cells during each time step and D_l is the solute diffusion coefficient in the liquid phase. Within a Δt_{macro}, the relationship between both time steps is $\Delta t_{micro} \leqq \Delta t_{macro}$.

4. Results and discussion

The Al-Cu alloy is chosen to simulate the several microstructures of dendritic growth in the present work with the material properties listed in table 1.
Free dendritic growth in an undercooled melt. In order to simulate free dendritic growth in an undercooled melt, the calculating domain is divided into 320×320 cells with a cell size of 0.2 μm, which is fine enough to resolve a dendrite tip radius (Zhu & Hong, 2001). The size is larger than the critical radius r^0 of a crystal, which is approximated by the following equation (Kurz & Fisher, 1998)

$$r^0 = (2\Gamma)/\left(\Delta T_{r^0}\right) \tag{16}$$

where Γ is the Gibbs-Thomson coefficient and ΔT_{r^0} is the undercooling for the occurrence of nucleation. Based on the calculation of the Gaussian distribution in the bulk liquid, the nucleation will appear if the simulated temperature is lowered by the amount of ΔT_{mn}. Thus, for simplicity, the mean nucleation undrecooling ΔT_{mn} in the bulk is used for ΔT_{r^0}. In the beginning of simulation, one nucleus with the preferential growth direction of 0^o or 45^o with respect to the horizontal direction is assigned in the center of the area. The initial concentration of the calculation domain is assumed to be C_0.
The simulated dendrite morphology of an Al-2.0mass%Cu alloy solidified into an undercooled melt is shown in Fig. 1 for three stages: (a) the initial growth stage before emitting the side branch, (b) the initial of the secondary arms emitting from the primary trunk, and (c) the dendrite morphology with well-developed secondary and even tertiary arms. The different levels of darkness in the figure indicate the concentration profiles in both the solid and liquid phases. Within the solid region, along the centerline of primary trunks or side arms, there exists a spine with lower concentration, which is considered as the result of the combined effect of curvature and interface kinetics (Warren & Boettinger, 1995). The concentration in solid near the solid-liquid interface shows the higher concentration where the final solidification occurs. It could be seen from Fig. 1 (c) that the tertiary arm branching occurs only at one side of the secondary arms. These phenomena have been consistent with the observation of experiments and also simulated by the modified cellular automaton (Fig. (d)-(f)) (Zhu & Hong, 2001) and phase field models (Warren & Boettinger, 1995). The results of Fig. 1 illustrates the similar capability of the model with the present modification to depict the dendrite evolution features, including the growing and coarsening of the primary trunk, the branching of the secondary and tertiary dendrite arms, as well as the solute segregation patterns.

T_l	Liquidus temperature [K]	928.0 (2mass%Cu) 922.0 (4.5mass%Cu)
T_m	Melting temperature [K]	933.0
k	Partition coefficient	0.17
m	Slope of the liquidus line [K/mass%]	-3.36
C_p	Specific heat [J/kg·K]	1086
ρ	Density [kg/m^3]	2780
λ	Thermal conductivity [W/m·K]	192.5
ΔH_v	Volumertic latent heat [J/m^3]	1.107×10^9
D_l	Solute diffusion coefficient in liquid [m^2/sec]	10^{-9}
D_s	Solute diffusion coefficient in solid [m^2/sec]	10^{-12}
Γ	Gibbs-Thomson coefficient [mK]	2.4×10^{-7}

Table 1. Thermal and physical properties of Al-Cu alloy (Zhu & Hong, 2001; Kurz & Fisher, 1998) used in the present calculation.

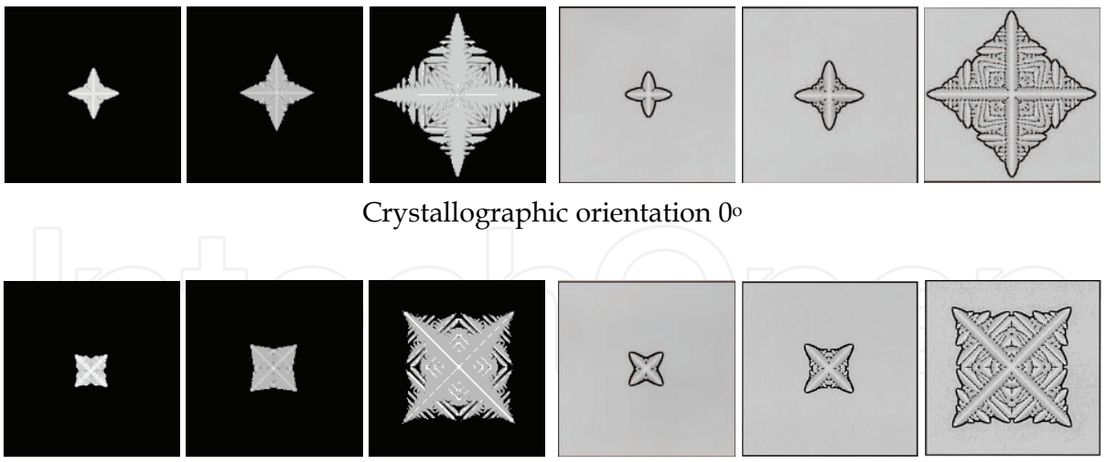

Fig. 1. The simulated dendritic shapes during the isothermal growth of an Al-2.0mass%Cu alloy

Prediction of the Structures formed in the directional solidification. The present model is applied to predict the evolution of dendritic grain structures of Al-2.5mass%Cu and Al-4.5mass%Cu alloys unidirectionally solidified over a copper chill plate with a constant temperature of 298 K. the nucleation parameters are listed in table 2. The symbols indexed "s" and "b" correspond to nucleation parameters on the mold surface and in the bulk liquid, respectively. Fig. 2 indicates the simulated and experimental macro- and micro- structures of Al-Cu alloys unidirectionally solidified with a pouring temperature of 1013 K. Fig. 2(c) and 2(f) indicate the simulated structures by the proposed method and Fig. 2(a), 2(b), 2(d) and 2(e) the experimental ones (Zhu & Hong, 2001). The left three figures indicate the case of the Al-2.5mass%Cu and the others for the case of the Al-4.5mass%Cu. Fig. 2(c) and 2(f), indicating the dendritic structures simulated by the proposed method, are also in good agreement with 2(c) and 2(f). The case of Al-4.5mass%Cu has smaller undercooling in the

	$n_{max,s}$ [m^{-2}]	$\Delta T_{mn,s}$ [K]	$\Delta T_{\sigma,s}$ [K]	$n_{max,b}$ [m^{-3}]	$\Delta T_{mn,b}$ [K]	$\Delta T_{\sigma,b}$ [K]
Al-2.5mass%Cu	1.8×10^{8}	0.5	0.1	8×10^{9}	5.0	0.1
Al-4.5mass%Cu	1.8×10^{8}	0.5	0.1	1.6×10^{10}	2.0	0.1

Table 2. The nucleation parameters of Al -Cu alloy (Zhu & Hong, 2001) used in the present calculation.

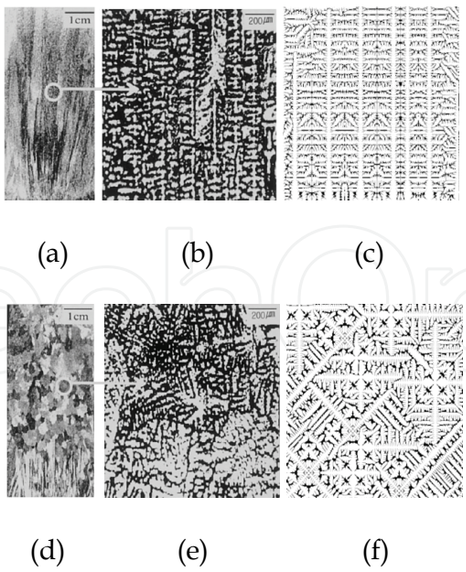

Fig. 2. Simulated and experimental results in directional casting of Al-Cu alloys.

bulk liquid, resulting in the nucleaction of equiaxed structures. For this simulation, a calculation domain is divided into 400×400 cells with a cell size of 3 μm, which is larger than the critical radius calculated by Eq. (16). It is seen that the proposed method can be applied to predict both the columnar and equiaxed dendritic morphology in a casting process of a binary alloy.

5. Conclusions

The proposed model, which is based upon the coupling of a modified cellular automaton model with the growth calculation of a nucleus in a given nucleation cell, has been developed to simulate the evolution of the dendritic structure in solidification of alloys. For a free dentritic growth in the undercooled melt, it is found that the proposed model can quantitatively describe the evolution of dendritic growth features, including the growing and coarsening of the primary trunks, the branching of the secondary and tertiary dendrite arms, as well as the solute segregation patterns. Moreover the directional solidification with the columnar and equiaxed grains is simulated by the proposed method and the evolution from nucleation to impingement between grains is observed.

6. References

Beltran-Sanchez, L. & Stefanescu, D. M. (2003). Growth of solutal dendrites: A cellular automaton model and its quantitative capabilities. *Metall. Mater. Trans. A*, Vol. 34A, p367-382.

Boettinger, W. J.; Warren, C.; Beckermann, C. & Karma, A. (2001). Phase-field simulation of solidification. *Annu. Rev. Mater. Res.*, Vol. l32, p163-194.

Gandin, Ch.-A.; Desbiolles, J.-L.; Rappaz, M. & Thevoz, Ph. (1999). A three-dimensional cellular automaton-finite element model for the prediction of solidification grain structures. *Metall. Mater. Trans. A*, Vol. 30A, No. 12, p3153-3165.

Juric, D. & Tryggvason, G. (1996). A front-tracking method for dendritic solidification. *J. Comput. Phys.*, Vol. 123, p127-148.

Kurz, W. & Fisher, D. J. (1998). *Fundamentals of Solidification*, Trans Tech Publication, Switzerland.

Kurz, W.; Giovanola, B. & Trivedi, R. (1986). Theory of Microstructural Development during Rapid Solidification. *Acta Metall.*, Vol. 34, p823-830.

Nastac, L. (1999). Numerical modeling of solidification morphologies and segregation patterns in cast dendritic alloys. *Acta Mater.*, Vol. 47, p4253-4262.

Rappaz, M. & Gandin, Ch.-A. (1993). Probabilstic modeling of microstructure formation in solidification processes. *Acta Metall. Mater.*, Vol. 41, No. 2, p345-360.

Sasikumar, R. & Sreenivasan, R. (1994). 2-dimensional simulation of dendrite morphology. *Acta Metall. Mater.*, Vol. 42, No. 7, p2381-2386.

Warren, J. A. & Boettinger, W. J. (1995). Prediction of dendritic growth and microsegregation patterns in a binary alloy using the phase-field method. *Acta Metall. Mater.*, Vol. 43, p689-703.

Zhu, M. F. & Hong, C. P. (2001). A modified cellular automaton model for the simulation of dendritic growth in solidification of alloys. *ISIJ Int.*, Vol. 41, No. 5, p436-445.

Cellular Automata - Innovative Modelling for Science and Engineering

Edited by Dr. Alejandro Salcido

ISBN 978-953-307-172-5
Hard cover, 426 pages
Publisher InTech
Published online 11, April, 2011
Published in print edition April, 2011

Modelling and simulation are disciplines of major importance for science and engineering. There is no science without models, and simulation has nowadays become a very useful tool, sometimes unavoidable, for development of both science and engineering. The main attractive feature of cellular automata is that, in spite of their conceptual simplicity which allows an easiness of implementation for computer simulation, as a detailed and complete mathematical analysis in principle, they are able to exhibit a wide variety of amazingly complex behaviour. This feature of cellular automata has attracted the researchers' attention from a wide variety of divergent fields of the exact disciplines of science and engineering, but also of the social sciences, and sometimes beyond. The collective complex behaviour of numerous systems, which emerge from the interaction of a multitude of simple individuals, is being conveniently modelled and simulated with cellular automata for very different purposes. In this book, a number of innovative applications of cellular automata models in the fields of Quantum Computing, Materials Science, Cryptography and Coding, and Robotics and Image Processing are presented.

InTech Europe
University Campus STeP Ri
Slavka Krautzeka 83/A
51000 Rijeka, Croatia
Phone: +385 (51) 770 447
Fax: +385 (51) 686 166
www.intechopen.com

InTech China
Unit 405, Office Block, Hotel Equatorial Shanghai
No.65, Yan An Road (West), Shanghai, 200040, China
中国上海市延安西路65号上海国际贵都大饭店办公楼405单元
Phone: +86-21-62489820
Fax: +86-21-62489821

IntechOpen